Systems & Control Transactions

Research Article
Foundations of Computer Aided Process Design (FOCAPD 2024)
Breckenridge, Colorado, USA. July 14-18, 2024
Peer Reviewed Conference Proceeding

PSE PRESS

Integration of Design and Operation with Discretization Error Control

Christian Hoffmann[a]*, Erik Esche[a], and Jens-Uwe Repke[a]

[a] Technische Universität Berlin, Process Dynamics and Operations Group, Berlin, Germany
* Corresponding Author: c.hoffmann@tu-berlin.de.

ABSTRACT

Optimization-based process design is a central task of process systems engineering. However, solely relying on steady-state models may potentially lead to dynamic constraint violations, hinder robust performance, or simply reduce the controllability of a process. This has led to the consideration of process dynamics in the design phase, which is commonly termed integration of design and operation / control. Recently, we proposed a framework to carry out this integrative task by formulating a large-scale nonlinear programming problem that is solved simultaneously. To this end, the dynamic process model was discretized, and dynamic variability and parametric uncertainty were included. However, the proposed framework only operates on constant lengths of the finite elements. The discretization error was not assessed. Within this contribution, a method for quantifying this discretization error and adapting the number of finite elements accordingly is incorporated into the recently proposed framework and applied on the case study of a continuous tank reactor. The obtained results with and without discretization error control are compared and, based thereon, a more suitable way to apply the control variables on the process is proposed.

Keywords: Integration of design and operation, Process design, Grid refinement, Nonlinear programming

INTRODUCTION

Process design is a central task of process systems engineering. This is conventionally achieved by using flowsheet simulators or other software to determine a suitable flowsheet. Based on this flowsheet, the process is designed using methods such as sensitivity analysis. A possible alternative is optimization-based process design in which the whole flowsheet is optimized for a given objective function. Both approaches typically rely on assumptions of stationarity. However, simply relying on steady-state models may potentially lead to dynamic constraint violations, hinder robust performance, or simply reduce the controllability of a process [1]. This has led to the consideration of process dynamics in the design, which is commonly termed integration of design and operation / control (IDO). Among the approaches to solving IDO problems is the dynamic optimization approach, which assesses the problem using rigorous dynamic models, and the robust approach, which ensures that no constraint violations occur at any point in time. For more information on the possible approaches to solving IDO problems, the reader is referred to the literature [1,2]. In recent years, we have proposed a framework for the solution of IDO problems, which can be seen as a hybrid of the dynamic optimization approach and the robust approach. The concept is based on a full discretization of the dynamic problem via orthogonal collocation, which yields a large-scale nonlinear programming problem [3]. The framework was then extended to account for parametric uncertainty [4] and to a larger case study [5]. Note that we limit ourselves to deterministic solutions in this contribution. The extension to optimization under uncertainty is, however, straightforward.

So far, the proposed framework has considered a constant number and length for the finite elements in the discretized dynamic model, which may potentially introduce notable discretization errors. Therefore, this contribution addresses this drawback by adding a method for quantifying and controlling the integration error. The extended framework is applied on a case study containing a continuously stirred tank reactor (CSTR) for which previous results are available so that the former and the new approach can be compared fairly.

STATUS QUO OF THE IDO FRAMEWORK

The current formulation of the IDO problem reads as follows [6]:

$$\min_{d,u_{cp,fe,sp}} \mathbb{E}\left[f\left(d,u_{cp,fe,sp},x_{cp,fe,sp},\xi_{sp},\nu_{cp,fe}\right)\right] \quad (1)$$

s.t.

$$0 = g\left(d,u_{cp,fe,sp},x_{cp,fe,sp},\xi_{sp},\nu_{cp,fe}\right) \quad (2)$$

$$0 \leq \mathrm{h}\left(\mathrm{d},\mathrm{u}_{cp,fe,sp},\mathrm{x}_{\mathrm{cp,fe,sp}},\xi_{\mathrm{sp}},\upsilon_{\mathrm{cp,fe}}\right) \quad (3)$$

$$0 = \mathrm{h}_0\left(\mathrm{d},\mathrm{u}_{0,sp},\mathrm{x}_{0,sp},\xi_{\mathrm{sp}},\nu_0,\mathrm{t}_0 = 0\right) \quad (4)$$

$$0 = \mathrm{h}_\mathrm{t}\left(\mathrm{d},\mathrm{u}_{t,sp},\mathrm{x}_{\mathrm{t,sp}},\xi_{\mathrm{sp}},\nu_\mathrm{t},\mathrm{t}_t\right) \quad (5)$$

$$\mathrm{d} \in \mathcal{D} \quad (6)$$

$$\mathrm{u}_{cp,fe,sp} \in \mathcal{U} \quad (7)$$

$$\mathrm{x}_{cp,fe,sp} \in \mathcal{X} \quad (8)$$

$$\nu_{cp,fe} \in \mathrm{APRBS} \quad (9)$$

$$\nu_{cp,fe} \sim \mathcal{N}(\mu,\Sigma) \quad (10)$$

Therein, the expected value of the objective function is minimized by varying the design *d* and the control variables *u* at all collocation roots *cp*, every finite element *fe*, and for all sigma points of the uncertainty space *sp*. The constraints include the dynamic process model *g*, path constraints, initial and terminal constraints h_0 and h_t. The variability of dynamic inputs is represented by an amplitude-modulated pseudo-random binary sequence (APRBS) [7] with normally distributed amplitude whereas the uncertain parameters ξ and the resulting probability density function of the uncertain inequality constraints, i.e., chance constraints, are represented by a point estimation method, e.g., a cubature rule. All design, state, and control variables are defined on their respective domain. The problem is solved simultaneously as large-scale nonlinear problem in Python, which is interfaced with the model formulation in AMPL [8] and the optimization algorithm IPOPT [9] via AmplPy.

METHODOLOGY

We now describe the theoretical basis of the error calculation. Afterwards, the solution of the optimization problem is sketched, including the initialization of the new variables that appear due to the increasing number of finite elements. Afterwards, the case study in this contribution is outlined.

Error calculation

There are several options to assess the discretization error. In many situations, one can compare the error between a highly resolved solution and the solution obtained with the current mesh grid to find an appropriate number of finite elements [10,11]. While this might be suitable for the solution of a standard boundary value problem, the additional challenge of this work are the relatively long time horizons and the additional degrees of freedom in terms of the design variables of the process. As a results, the highly resolved solution might require significant computational effort and careful initialization. To avoid that, we chose an error estimation that does not compare the difference between two solutions, but the residual between the left-hand and the right-hand side of the differential equations. This estimation of the discretization error is based on the work by Chen et al. [12,13]. In their first publication, they formulated the search for an appropriate number and length of the finite elements as a bilevel optimization problem. As they pointed out, this entails significant computational demand [12]. Hence, they proposed in their subsequent publication to estimate the discretization error by evaluating the residual of the orthogonal collocation T_{fe} [13]:

$$T_{i,fe} = \frac{\mathrm{d}x_i}{\mathrm{d}t}\left(t_{fe,nc}\right) - \Delta t_{fe} f\left(x,u,d,t_{fe,nc}\right). \quad (11)$$

Therein, the residual for the i-th state variable is evaluated at one (or several) non-collocation points (subscript nc), i.e., points different from the used Radau roots. In their approach, Chen et al. also included the residuals of the algebraic equations. Here, we limit ourselves to the differential equations of the model although the extension to algebraic equations is straightforward. Based on the residual, the discretization error is estimated as:

$$err_{i,fe} = \mathrm{C}\left\|T_{i,fe}\right\|. \quad (12)$$

The constant C is given by the following integral:

$$\mathrm{C} = \frac{1}{A}\int_0^{\tau_{fe,nc}} \prod_{j=1}^{K}\left(s-\tau_j\right)\mathrm{d}s\,, \quad A = \prod_{j=1}^{K}\left(\tau_{fe,nc}-\tau_j\right) \quad (13)$$

This constant only depends on the choice of the non-collocation point(s) and the type of collocation points (in this case Radau) and can thus be calculated once at the beginning. The discretization error must be smaller than a user-defined tolerance:

$$err_{i,fe} \leq \mathrm{tol}_i \quad (14)$$

A similar scheme was recently proposed in [14].

Solution

The algorithmic approach of this contribution is as follows: First, the optimization problem above is initialized, e.g., via a steady-state optimization. Afterwards, the dynamic system is added, and dynamic variability of the inputs is introduced. Then, the optimization problem is solved by minimizing the objective using a nonlinear optimization algorithm, in this case IPOPT [9]. Based on the obtained results, the discretization error is calculated as described in Equations (12) and (13). If the error within one finite element is larger than the tolerance, the

respective finite element is split into two. These two finite elements are now initialized based on the current solution. This could be done via simple linear interpolation, but as we use collocation, the new initial guesses are calculated by evaluating the Lagrange interpolation polynomial, i.e., the sum of the Lagrangian basis polynomials of the collocation, at the new collocation points. This is repeated for all finite elements. Both approaches to initialize the finite elements have their advantages and disadvantages. For the simple case study below, both would probably work equally well. Finally, the optimization problem is solved again and the error calculation is repeated. This step continues until all errors of the finite elements are smaller than the set tolerance.

Case study

The case study is a CSTR as shown in Figure 1. Component A enters the reactor via the volume flow q_F and reacts to B. The volume flow q then leaves the system with concentration c_A and temperature T. The feed flow and the feed temperature are assumed as variable, dynamic inputs. The cooling duty Q_C can be manipulated with cooling water whose stream is change via the valve position VP_1. The outlet flow can be manipulated using valve position VP_2.

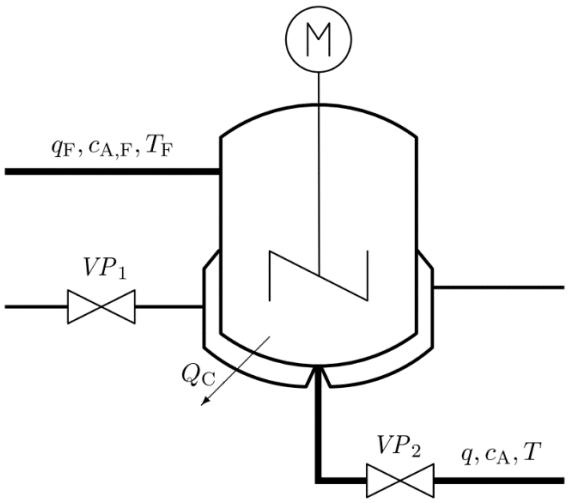

Figure 1. Flowsheet of the CSTR in this case study [6].

For the process model, the following three assumptions are made [6]:

1. Density and heat capacity of the flows are constant and thus independent of temperature, pressure, or composition.
2. The liquid phase in the reactor is ideally mixed.
3. The pressure remains constant during operation.

This results in the following mass, component, and energy balances:

$$\frac{\mathrm{d}V^L_{\mathrm{CSTR}}}{\mathrm{d}t} = q_F - q \tag{15}$$

$$\frac{\mathrm{d}c_A}{\mathrm{d}t} = \frac{q_F}{V^L_{\mathrm{CSTR}}}\left(c_{A,F} - c_A\right) - k_0 \exp\left(-\frac{E}{RT}\right) c_A \tag{16}$$

$$\frac{\mathrm{d}T}{\mathrm{d}t} = \frac{q_F}{V^L_{\mathrm{CSTR}}}(T_F - T) + k_0 \exp\left(-\frac{E}{RT}\right) c_A(-\Delta_R h) - \frac{\dot{Q}_C}{\rho c_P V^L_{\mathrm{CSTR}}} \tag{17}$$

Therein, k_0 and E are the pre-exponential factor and the activation energy of the reaction, respectively, $\Delta_R h$ is the enthalpy of reaction, ρ is the density, and c_p is the heat capacity. Moreover, the cooling duty is a function of VP_1, whereas the liquid outlet depends on the liquid volume within the reactor and VP_2. The operating costs depend on the outgoing mole flow of component A, the investments costs depend on the diameter and the height of the CSTR. The objective function is the sum of both costs. The control variables can be changed from one collocation point to another. However, this change is bounded:

$$\|u(t_i) - u(t_{i+1})\| \leq \Delta u_{\max} \tag{15}$$

The maximum change of u is specified by the user. We call this control formulation 1. For the temperature, an upper bound of 480 K is specified. Not violating this upper bound must be ensured by the process design in combination with the allowable range of the control variables. More details on the equations and the specifications for mean and standard deviation of the dynamic variability of feed flow and feed temperature can be found in [6].

For the results shown below, 0.5 was chosen as non-collocation point based on the work by Chen et al. [13], and a tolerance of 0.1 was specified for the discretization error. This value will be critically discussed at the end of the following section.

RESULTS AND DISCUSSION

The proposed optimization problem in combination with the method for quantifying the discretization error was solved for the presented case study. The obtained dynamic profiles are shown in Figure 2 (top). It can be observed that the temperature (black continuous line) is very close to but below the upper bound, meaning the IDO problem was solved successfully. In blue, the variation of the feed temperature is shown as a result of the APRBS. Lastly, the gray curve visualizes the change of the control variable VP_1. For comparison, the obtained temperature profile with fixed number and length of finite elements is shown [6]. We frequently observe situations in which the temperature lies below the upper bound (where conversion is the largest) to ensure that the process can be sufficiently cooled.

Figure 2 (bottom) shows, however, the negative impact of the refined discretization scheme. As more and more very small finite elements appear, these elements

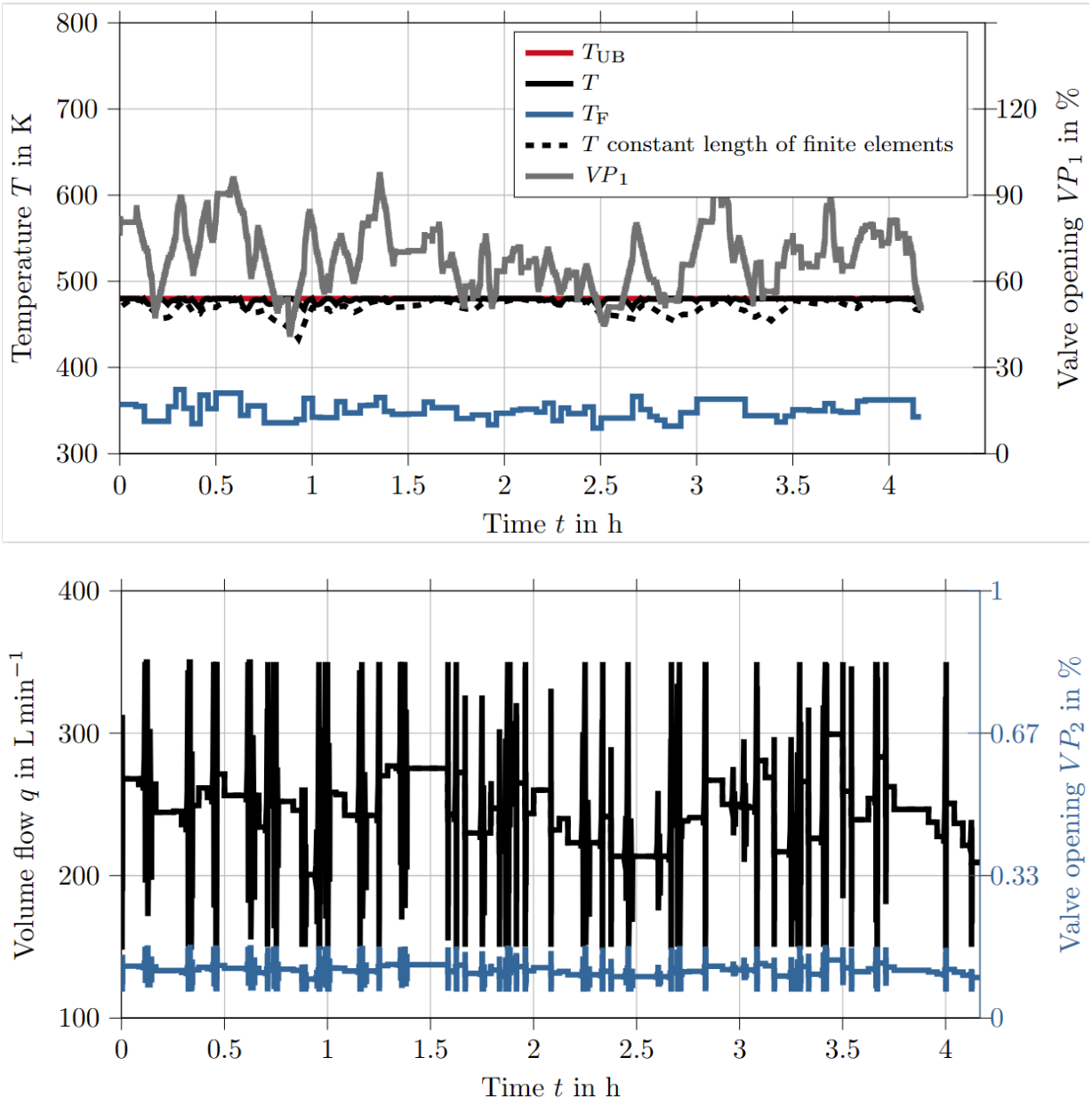

Figure 2: Dynamic profiles for temperature and opening of valve 1 (top), volume flow and opening of valve 2 (bottom) for control formulation 1, i.e., control variables change between collocation points and can change by a certain range. Also included in the top figure is the dynamic feed temperature, the upper bound of the temperature during operation, and the temperature profile obtained for constant number and length of the finite elements [6].

allow the same control changes as longer elements. This results in very undesirable bang-bang solutions for the volume flow from the reactor, which would be deemed unrealistic (at best) or would render the process inoperable in practice. As a result of these observations, an alternative formulation had to be found that allowed a varying length of finite elements but also a generically applicable bound on the control changes. For this reason, control formulation 2 is proposed:

$$\frac{\mathrm{d}u_{i,fe}}{\mathrm{d}t} = u_{\mathrm{ramp},i,fe} \text{ with } \left\|u_{\mathrm{ramp},i,fe}\right\| \leq u_{\mathrm{ramp,max,i}} \qquad (18)$$

This means that the control variables are linear functions in each finite element. In addition, the control profiles must be continuous, i.e., the endpoint of control i in finite element fe is equal to the starting point of control i in finite element fe+1. For this control formulation, the IDO

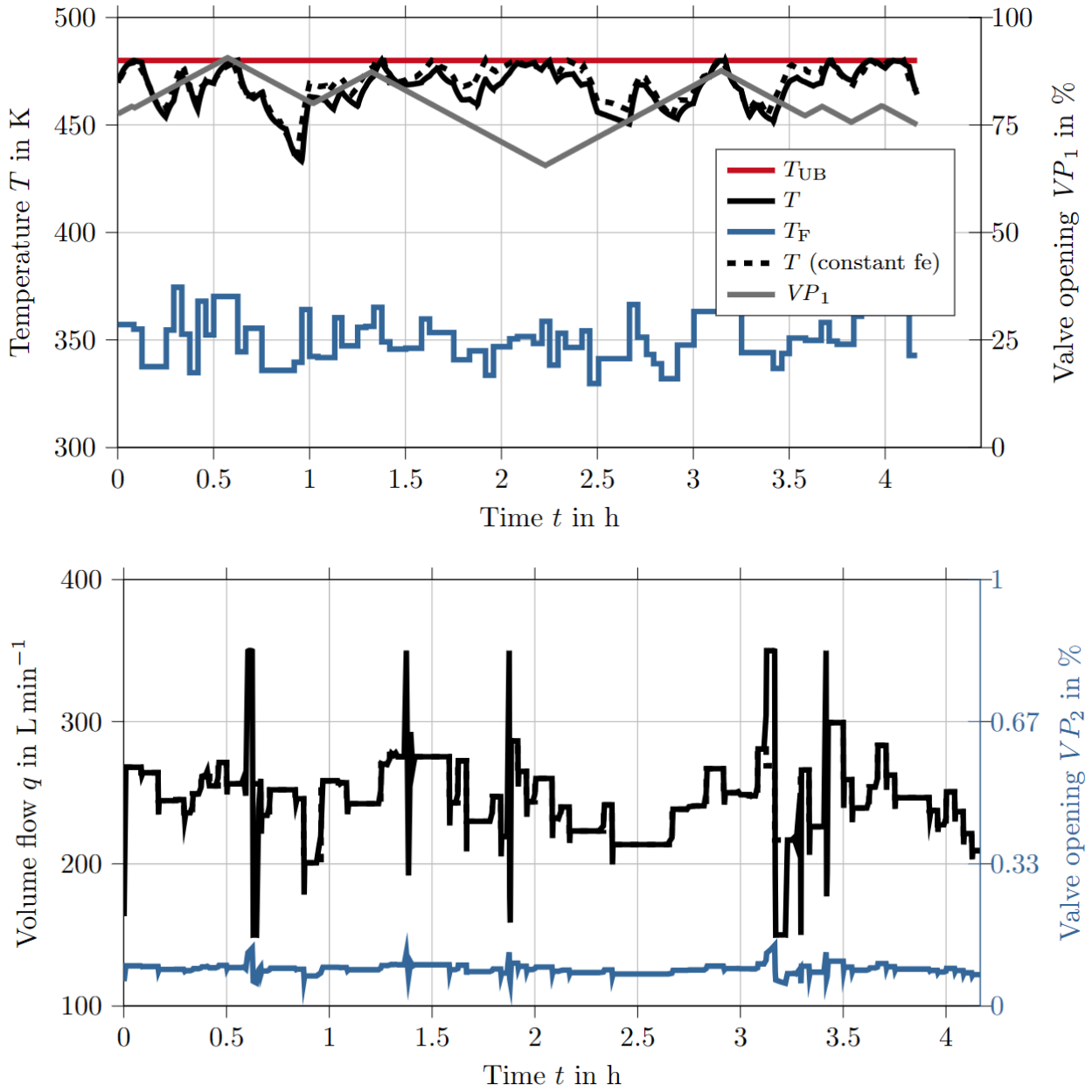

Figure 3: Dynamic profiles for temperature and opening of valve 1 (top), volume flow and opening of valve 2 (bottom) for control formulation 2, i.e., control variables change linearly within one finite element and their change rate is constrained. Also included in the top figure is the dynamic feed temperature, the upper bound of the temperature during operation, and the temperature profile obtained for constant number and length of the finite elements (constant fe) [5].

problem was solved again. The results are shown in Figure 3. The temperature profile is now much closer to the original solution with fixed number and length of the finite elements. The difference is, of course, that the number of finite elements is now much higher (here: 451 instead of 50) and that the profiles of the control variables are linear function in every finite element. In consequence, the IDO problem is successfully solved as well, but does not show the bang-bang solutions of control formulation 1 (Figure 3, bottom). We conclude that the approach of linearizing the control profiles is suitable in the context of this contribution in which the process design can change to make the process resilient with respect to sudden changes in inputs, such as feed flows. We would necessarily recommend this approach for other applications, such as parameter estimation.

Table 1: Design specifications and cost functions for steady-state solution, dynamic solution with fixed number and length of finite elements ("previous solution", taken from [6]), and dynamic solutions with control formulation 1 and 2. The investment costs are given as annuity.

Variable	Unit	Steady-state solution [6]	Previous solution [6]	Control formulation 1	Control formulation 2
V_{CSTR}	m^3	$4.58 \cdot 10^{-1}$	$7.31 \cdot 10^{-1}$	$4.86 \cdot 10^{-1}$	$8.10 \cdot 10^{-1}$
d_{CSTR}	m	$5.26 \cdot 10^{-1}$	$6.15 \cdot 10^{-1}$	$5.37 \cdot 10^{-1}$	$6.37 \cdot 10^{-1}$
L_{CSTR}	m	$2.11 \cdot 10^{0}$	$2.46 \cdot 10^{0}$	$2.15 \cdot 10^{0}$	$2.55 \cdot 10^{0}$
C_{inv}	\$ y^{-1}	$2.21 \cdot 10^{+2}$	$4.70 \cdot 10^{+2}$	$3.65 \cdot 10^{+2}$	$5.01 \cdot 10^{+2}$
C_{op}	\$ y^{-1}	$3.51 \cdot 10^{+2}$	$2.29 \cdot 10^{+2}$	$2.17 \cdot 10^{+2}$	$2.38 \cdot 10^{+2}$
f	\$ y^{-1}	$5.72 \cdot 10^{+2}$	$6.99 \cdot 10^{+2}$	$5.82 \cdot 10^{+2}$	$7.39 \cdot 10^{+2}$

It should be noted here that the approach might benefit from techniques to combine finite elements again where the discretization error is significantly below the set tolerance as, for example, described by Liu et al. [11], to keep the computational effort as low as possible. However, repeatedly adding and removing finite elements could potentially slow down convergence of the overall design problem, which is why this has not yet been implemented.

Table 1 compares the design results of our previous study [6] and the results of this work. The smallest reactor volume is still found for the steady-state case as this solution does not have to account for dynamic variability. The solution obtained for control formulation 1 results in a smaller reactor volume (and a smaller objective function) as the short-finite elements provide much more flexibility of the control variables at the cost of bang-band solutions. Control formulation 2 results in a larger reactor volume. This might be due to the combination of the linear profiles for the control variables, but also because constraint violations hidden in the previous solution are now removed because of the controlled discretization error. Lastly, the role of the non-collocation point used for quantifying the discretization error shall be discussed.

Table 2: Necessary number of finite elements under variation of the non-collocation point for control formulation 2. The case at 0.9 automatically satisfies the condition because C is negative and thus the error is automatically smaller than zero.

Non-collocation point	Constant C	Number of finite elements
0.1	0.2250	368
0.4	0.0000	50
0.5	0.1250	305
0.6	0.6000	355
0.9	-0.0592	50

The very pronounced increase of the necessary finite elements by a factor of about 10 was very surprising, given that the system is not very complex. Hence, the specific location of the non-collocation point was varied to determine how the number of finite elements changes (Table 2). It is observed that the location of the non-collocation point has a notable effect on the necessary number of finite elements. Specifically, the constant C has roots in the interval from zero to one (so the discretization error estimate is automatically zero as well), and it can become negative for non-collocation points closer to one. Hence, better criteria for its selection must be found. Until now, this remains and open research question and has, to the author's knowledge, not been discussed so far in other contributions.

The impact of the continuously refined mesh is visualized in Figure 4. The design starts off with a reactor volume of 0.84 m^3 and declines to approximately 0.81 m^3 (see also Table 1). Although this impact is (in this case small) relatively small, it shows that it should still be investigated, especially for larger flowsheets with varying time constants. For the objective function, however, there is no clear trend observable (Figure 5).

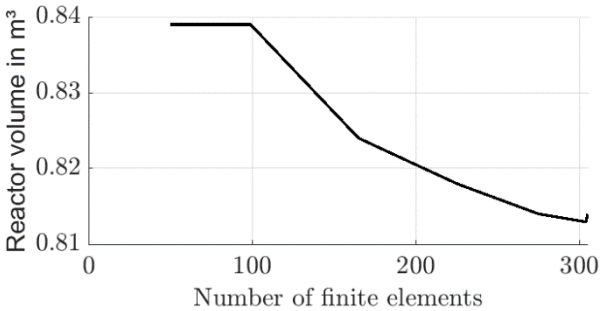

Figure 4. Reactor volume with increasing number of finite elements for a non-collocation point of 0.5.

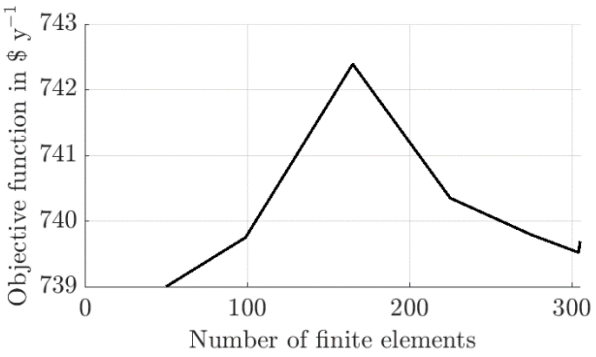

Figure 5. Objective function with increasing number of finite elements for a non-collocation point of 0.5.

CONCLUSION AND OUTLOOK

This contribution extended our recently proposed framework for solving IDO problems by incorporating a measure of the discretization error to avoid incorrect profiles and, in consequence, possibly hidden constraint violations in these badly resolved regions. The extended framework was applied on a CSTR case study for which its geometry, i.e., volume, height, and diameter, was determined while satisfying operational constraints, such as an upper bound of the temperature, for all timepoints in the horizon. Based on the presented findings, a reformulation for control variables is recommended, i.e., the linearization of the profiles within one finite element, which prohibits strongly oscillating control profiles in highly resolved regions of the time horizon.

In the future, this error-controlled approach shall be extended to parametric uncertainty. This is of particular interest as the probability distribution of the uncertain parameters will influence the time constants of the individual scenarios, which will potentially result in completely different numbers and lengths of the finite elements for each uncertainty scenario.

REFERENCES

1. Ricardez-Sandoval LA, Budman HM, Douglas PL. Integration of design and control for chemical processes: A review of the literature and some recent results. *Annu Rev Control* 33:158–171 (2009).
2. Vega P, Lamanna de Rocco R, Revollar S, Francisco M. Integrated design and control of chemical processes – Part I: Revision and classification. *Comput Chem Eng* 71:602–617 (2014).
3. Hoffmann C, Esche E, Repke J-U. Integration of design and control based on large-scale NLP formulations and an optimal economic NMPC. In: Proceedings of the 9th International Conference on Foundations of Computer-Aided Process Design. Ed: Garcia Munoz S, Laird CD, Realff MJ. Elsevier (2019).
4. Hoffmann C, Weigert J, Esche E, Repke J-U. Integration of design and operation using dynamic perturbation and chance constraints with unscented transform. In: 30th European Symposium on Computer Aided Process Engineering. Ed: Pierucci S, Manenti F, Bozzano GL, Manca D. Elsevier (2020).
5. Hoffmann C, Esche E. Integration of design and operation for the CO2-based methanol synthesis. In: 14th International Symposium on Process Systems Engineering (PSE 2021+). Ed: Yamashita, Yoshiyuki, Kano, Manabu. Elsevier - Health Science (2022).
6. Hoffmann C. A Framework for the Integration of Design and Operation under Uncertainty Using Dynamic Perturbation and Chance Constraints. Dissertation. Technische Universität Berlin, Germany (2023).
7. Nelles O. Nonlinear System Identification. Springer (2001).
8. Fourer R., Gay D. M., Kernighan B. W. AMPL: A Modeling Language for Mathematical Programming. Duxbury Thomson (2002).
9. Wächter A, Biegler LT. On the implementation of an interior-point filter line-search algorithm for large-scale nonlinear programming. *Math. Program.* 106:25–57 (2006).
10. Ascher U. M., Petzold L. R. Computer methods for ordinary differential equations and differential-algebraic equations. Society for Industrial and Applied Mathematics (1998).
11. Liu F, Hager WW, Rao AV. Adaptive mesh refinement method for optimal control using nonsmoothness detection and mesh size reduction. *Journal of the Franklin Institute* 352:4081–4106 (2015).
12. Chen W, Biegler LT. Nested direct transcription optimization for singular optimal control problems. *AIChE J* 62:3611–3627 (2016).
13. Chen W, Ren Y, Zhang G, Biegler LT. A simultaneous approach for singular optimal control based on partial moving grid. *AIChE J* 65:e16584 (2019).
14. Palma-Flores O, Ricardez-Sandoval LA. Selection and refinement of finite elements for optimal design and control: A Hamiltonian function approach. *AIChE J* 69:e18009 (2023).